International Journal of Recent Technology and Engineering (IJRTE)
ISSN: 2277-3878 (Online), Volume-9 Issue-2, July 2020

Performance Examination of Low-Power Thermoelectric Sensor Arrays for Energy Harvesting From Human Body Heat

Law Choon Chuan, Herman Wahid, Dirman Hanafi, Seriaznita Haji Mat Said

Abstract*: *Thermoelectric energy harvester is known as a type of energy harvesting technologies which extracts waste heat from a target device or object to generate electrical power. The low power generation from thermoelectric energy harvester, though, is always a critical consideration in designing a self-sustaining system. The energy harvesting system is usually aided by a power management solution to further enhance the power generation for better performance. Therefore, maximizing the power generated from the thermoelectric sensor itself is essential in order to select the most suitable power management approach. This paper presumed the methodology to maximize power generation of thermoelectric and further discussion is reviewed in the report.

Keywords* : *Thermoelectric, energy harvester, optimal array, performance, self-sustain system.

I. INTRODUCTION

Energy harvesting technologies utilize the ambient energy to generate electrical power. Nowadays, it is widely popular among the researchers studying to produce renewable green energy from the surrounding ambient since it does not harm the environment. . The technology is attractive because electrical power can be generated without the use of batteries as well as it provides an autonomous option for a self-sustaining power system.

The utmost important consideration for an energy harvesting technology is to have a stable supply of ambient energy source. When considering an ambient energy that is readily available for medical equipment, the very best option is heat source. Heat can be garnered from a live human body whereby an energy harvesting technology can be used to provide the autonomous stable power state for any medical devices. As stated in [1,8,9,10], a live human body provides a stable and continuous source of heat energy which can be extracted.

Thermoelectric generator (TEG) is one of energy harvesting devices which converts the temperature gradient to a usable electrical energy. TEG is a widely known sensor without any moving parts with a simple structure. Application of TEG in medical equipment fulfills the need for bionic sensor devices; convenient, maintenance free and with an unlimited supply of energy. Furthermore, an autonomous medical device that uses TEG reduces the risk of power outage during power plant's maintenance or genset generator failure [2,11,12].

The autonomous self-sustaining property, though, is mainly dependent on the power requirement of the system [2,15]. The higher the power requirement is, the more sensors' are required to generate electrical power to meet the supply and demand of the electricity. Fig. 1 illustrates the basic function of a thermoelectric sensor.

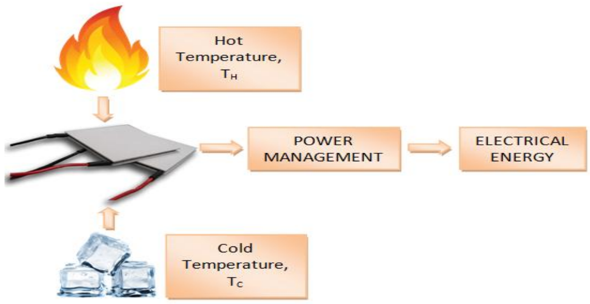

Fig. 1 Basic thermoelectric function block

The disadvantage of TEG in real world applications is when the energy conversion efficiency is relatively low. This research is on converting human body heat into an electrical energy, whereby the temperature difference is relatively small. Due to that, voltage produced is hardly adequate to power other systems. Taking into consideration Chen's earlier proposal, implantable medical sensors can be built in together with TEG sensors to complete a self-sustaining medical monitoring system [3]. From the studies, the power requirement for implantable sensors is shown in Fig. 2, whereby it seems possible to build TEG sensors together with these sensors with power consumption from 1 µW up to 2 mW. Since a single TEG is only able to produce a very small amount of power, it is possible to design and assemble the sensors in array configurations. However, it is difficult to ensure that every sensor will work under the same specifications [4,15].

Manuscript received on May 25, 2020.
Revised Manuscript received on June 29, 2020.
Manuscript published on July 30, 2020.
* Correspondence Author
Law Choon Chuan, Universiti Teknologi Malaysia, Johor, Malaysia., Email: kumarun_87@yahoo.com
Herman Wahid*, Universiti Teknologi Malaysia, Johor, Malaysia.. Email: herman@utm.my
Dirman Hanafi, Universiti Tun Hussien Onn Malaysia, Johor, Malaysia. Email: dirman@uthm.edu.my
Seriaznita Haji Mat Said, Universiti Teknologi Malaysia, Kuala Lumpur, Malaysia.. Email: seriaznita.kl@utm.my

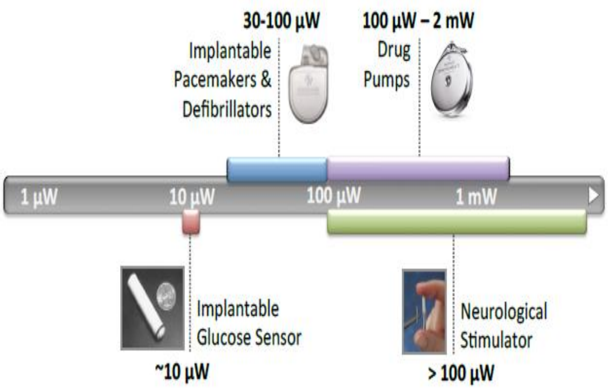

Fig. 2 Power requirements of implantable sensors [2]

In order to prove the feasibility of realizing this combined technology, an experimental review of the technology had been proposed and performed to reveal the performance of TEG sensor. A low power type of TEG sensor is selected and tested for various human body temperatures in order to ascertain the capabilities and performance of the sensor. This paper is structured as follows: Section 2 presents the methodology of the studies; Section 3 discusses series of experimental results; and finally Section 4 is a conclusion of the experiment.

II. TEG SENSOR SELECTION AND SPECIFICATIONS

A 0.8 W low power TEG sensor is selected from a local distributor in Malaysia to investigate its performance for various human body temperatures. The specification of the sensor is tabulated in Table 1.

Table 1 Specification of a 0.8W TEG sensor

Specifications	Measurements
Length (mm)	6
Width (mm)	4
Height (mm)	3
Maximum Current (A)	0.6
Maximum Voltage (V)	1.4
Maximum Power (W)	0.8
Maximum Changes of Temperature (°C)	73

The sensor is built up with two commonly used materials, bismuth telluride and bismuth antimony telluride. Each of the sensors is connected to 11 thermocouples in series. In order to ensure a smooth measurement process, the sensors is assembled and soldered within a small PCB board. The exact workpiece of the test board is depicted in Fig. 3.

Continuing with the measurement process, these sensors will undergo the measurement process for hot side temperature ranging from 30 °C to 40 °C while the cold side is exposed to the ambient temperature of the laboratory. The temperature on the hot side measured was about 37 °C which is similar to a temperature of a normal live human body (i.e. skin) in Malaysia. The body temperature could vary from 32 °C (for healthy person) and up to 40 °C (for fever case) [5]. Therefore, the temperature gradient for the hot and cold side is assumed to be from 5 to 15 °C.

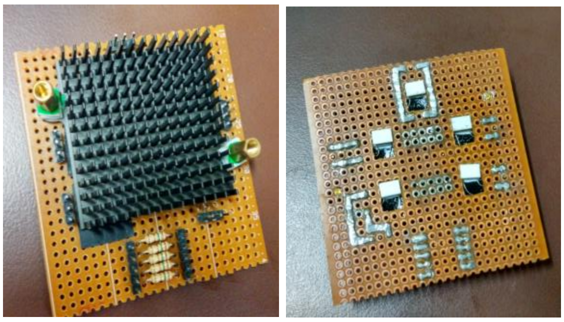

Fig. 3 Work Piece of 5 TEG sensors

For each of the temperature range, the sensors are arranged in order to monitor the performance from different configurations. The test is carried out utilizing a hot plate from Fisher Scientific (Model no. 1110250SH) as the temperature source for the hot side of the sensors. The photo of the hot plate is shown in Fig. 4. For the total of five sensors, all were configured in series, parallel and combination of both to identify the best performance for each of the temperature differences.

Fig. 4 Fisher Scientific Hot Plate

III. MEASUREMENT RESULTS

A. Single Sensor Performance

To measure the sensor, a PCB board is fixed at the center of the hot plate to obtain the optimum heat transfer. The test is performed by using a hot plate with a temperature range from 30 °C to 40 °C while the cold side of the sensor is exposed to the room temperature of about 27 °C. Voltage and current measurements was recorded and are tabulated in Table 2.

Each of the data is plotted into a graph to identify the characteristics of voltage, current and output power against the temperature difference, as shown in Fig. 5. It was determined that sensor number five produces higher power output when compared to others. From the graph, it is clearly seen that performance of the sensors are not quite linear from a parabolic function, except for the voltage-temperature characteristic in which linear relationship can be approximated using a best-fit line method and will be further analysed in this section. In the following sections, both series and parallel configurations are evaluated to monitor the changes of the sensor performances.

Table 2 Single Sensor Performance.

Sensor	ΔT (°C)	Vo (mV)	Io (mA)	Po (μW)
S1	7.4	4.7	0.52	2.44
	11.8	10.5	1.37	14.39
	16.4	15.1	2.75	41.53
S2	7.4	5.6	0.55	3.08
	11.8	9.3	1.51	14.04
	16.4	16.6	3.08	51.13
S3	7.5	4.5	0.47	2.12
	11.8	8.9	1.35	12.02
	16.4	15.9	2.74	43.57
S4	7.5	4.3	0.54	2.32
	11.8	8.4	1.25	10.50
	16.4	17.2	3.01	51.77
S5	7.5	4.2	0.52	2.18
	11.7	9.1	1.45	13.20
	16.4	18.2	2.90	52.78

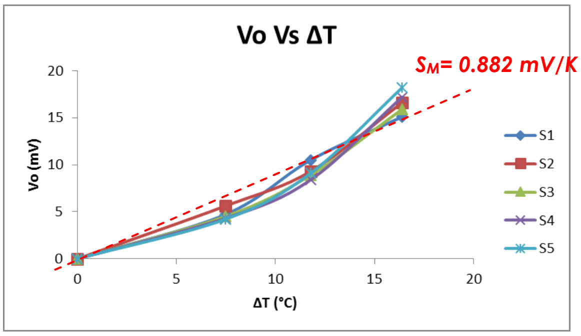

(a)

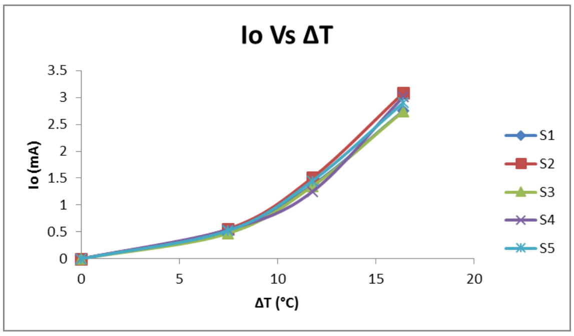

(b)

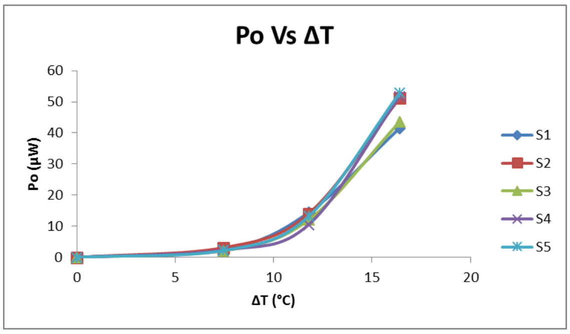

(c)

Fig. 5 Sensors' performance for (a) output voltage, (b) output current, and (c) output power against temperature differences

In addition, there are published data that are available as shown in [5] and [6] that can be used as references to identify if the performance of the sensors used in this experiment fall under standard performance class. From the graphs shown in Fig. 6 and 7, the performance of the sensors when compared with the ones from the previous study is rather identical in their plot pattern. Although the sensors used in both studies are dissimilar, the performance of the sensors produces similar non-linear plots. Therefore, it can be verified that the sensors used in this experiment perform under standard conditions.

By adopting the given parameters in Table 1, the Seebeck coefficient can be determined from the formula below [7]:

$$S_M = Vmax / Th \qquad (1)$$

where S_M is Seebeck coefficient of the module, *Vmax* is maximum voltage of sensor given in Table 1 and *Th* refers to hot side temperature in contact with the sensor. The result of the calculated Seebeck coefficient is tabulated in Table 3.

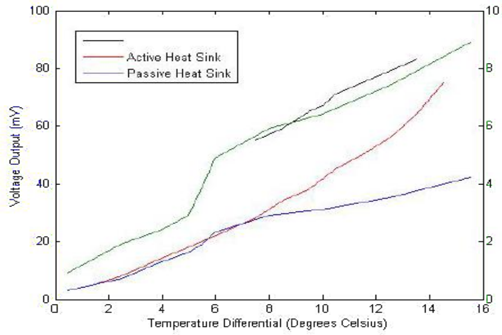

(a)

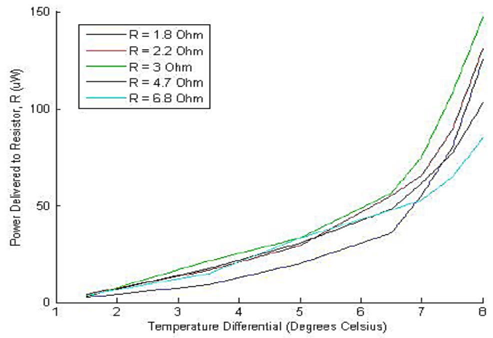

(b)

Fig. 6 Reference of TEG sensors performance for (a) output voltage, and (b) output power against temperature differences. [5]

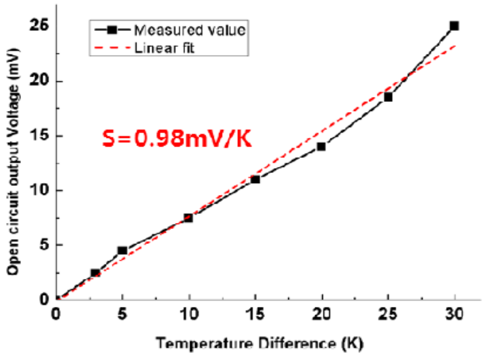

(a)

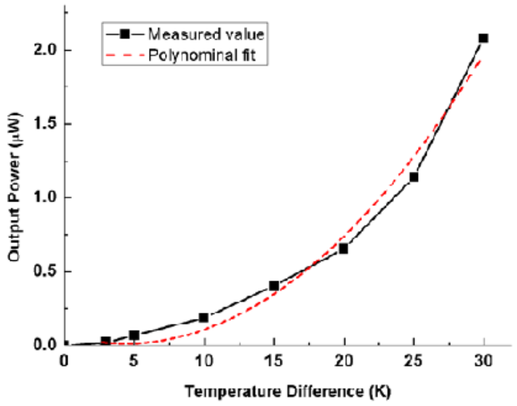

(b)

Fig. 7 Second reference of TEG sensors performance for (a) output voltage, and (b) output power against temperature differences [6]

The coefficient was then substituted into formula (2) to generate a series of output voltage at several temperature differences and then compared with the results measured from the experiment. Below is the description of formula (2), [7]:

$$V=S_M\Delta T+IR_M \qquad (2)$$

where V is the voltage generated by the sensor, S_M is the Seebeck coefficient, ΔT is the temperature difference between the hot and cold side of the sensor, I is the current measured for the temperature differences and R_M refers to resistance of the TEG module. Formula 3[7] below is used to calculate R_M,

$$R_M=(T_h-T_{max})V_{max}/T_hI_{max} \qquad (3)$$

The results for R_M calculated from the formula are shown in Table 4. The deviation for the calculated and measured output voltages are found to be very large ranging from 77 percent to 88 percent while the output voltage calculated from the vendor specification is much higher than the measured output voltage. In order to ensure the reliability of the measured data, the measured parameters are used in the configuration analysis for both series and parallel configurations.

Table 3 Theoretical (calculated) Seebeck coefficients.

Hot Temperature, T_h (°C, K)	V_{max} (V)	S_M (mV/K)
25°C / 298K	1.4	4.698

Table 4 The comparison results of output voltage between theoretical (calculated) and measurement methods.

Sensor	ΔT, K	Rm, Ω	Vo (cal), mV	Vo (meas), mV	%|error|
S1	7.4	1.32	35.45	4.7	86.8
	11.8	1.32	57.14	10.5	81.62
	16.4	1.32	80.67	15.1	81.29
S2	7.4	1.32	35.5	5.6	84.23
	11.8	1.32	57.43	9.3	83.21
	16.4	1.32	81.11	16.6	79.54
S3	7.5	1.32	35.85	4.5	87.45
	11.8	1.32	57.22	8.9	84.45
	16.4	1.32	80.66	15.9	80.29
S4	7.5	1.32	35.95	4.3	88.04
	11.8	1.32	57.09	8.4	85.29
	16.4	1.32	81.02	17.2	78.77
S5	7.5	1.32	35.92	4.2	88.31
	11.7	1.32	56.88	9.1	84
	16.4	1.32	80.88	18.2	77.5

The data for sensor 1 from Table 1 is then plotted into a linear graph as depicted in Fig. 8. The comparison of trend line shows that the deviation of the sensor's performance is very large when compared with the actual trend line. It is believed that the ambient of the test section affected the outcome since it was performed in an open area which allows numerous factors to affect the results, such as uncertain temperature dissipation. Nevertheless, the measured values will be adopted as it is the references for the configuration sections. Thus, it is believed that the sensors are operating under optimum conditions and the results produced are reliable.

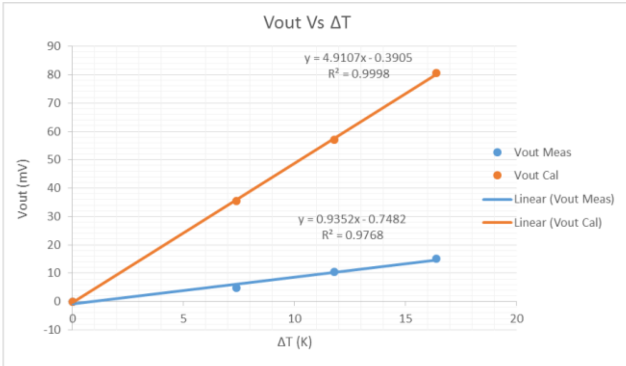

Fig. 8 Comparison of trend line for measured voltage (red) and calculated voltage using Seebeck coefficient (blue)

B. Series Performance

For the second configuration, the sensors are connected in series connection by two sensors, three sensors, four sensors and five sensors in sequential order. For the series connection, the voltage of the sensors is expected to sum up while the current remains unchanged. The series connection provides information whereby the maximum power produced is achieved by increasing the voltage ratings while the current rating is maintained at approximately the same level. The exact performance of series configuration is tabulated in Table 5(a)-(c) for different temperature differences and the performance curve is depicted in Figure 9.

Table 5(a) Sensor series configuration for temperature differences at 4.72 °C

No. of Sensor	ΔT (°C)	Vo (mV)	Io (mA)	Po (µW)
1	4.72	5.6	0.55	3.08
2	4.72	7.8	0.79	6.16
3	4.72	16.6	0.99	16.43
4	4.72	2.5	0.82	2.05
5	4.72	3.7	0.29	1.07

Retrieval Number: B3769079220/2020©BEIESP
DOI:10.35940/ijrte.B3769.079220
Journal Website: www.ijrte.org

Published By:
Blue Eyes Intelligence Engineering
& Sciences Publication

Table 5(b) Sensor series configuration for temperature differences at 9.63 °C

No. of Sensor	ΔT (°C)	Vo (mV)	Io (mA)	Po (μW)
1	9.63	10.5	1.37	14.39
2	9.63	18.0	1.88	33.84
3	9.63	21.0	2.48	52.08
4	9.63	41.0	2.58	105.78
5	9.63	39.4	2.65	104.41

Table 5(c) Sensor series configuration for temperature differences at 14.30 °C

No. of Sensor	ΔT (°C)	Vo (mV)	Io (mA)	Po (μW)
1	14.30	18.2	2.90	52.78
2	14.30	34.3	4.25	145.78
3	14.30	59.3	5.72	339.20
4	14.30	48.6	3.72	180.79
5	14.30	59.8	4.06	242.78

From the graphs shown in Fig. 9, it can be observed that the performance of the sensors is absolutely non-linear. This situation occurred during the measurement recording process when the cold side of the sensor is exposed to the ambient temperature in an air conditioned laboratory whereby the temperature changes slightly from time to time depending on the number of users in the room. Moreover, the heat dissipation for the hot plate starts from the center of the hot plate. Since the heat dissipation is not equally dissipated, the heat received by each of the sensors differs as well.

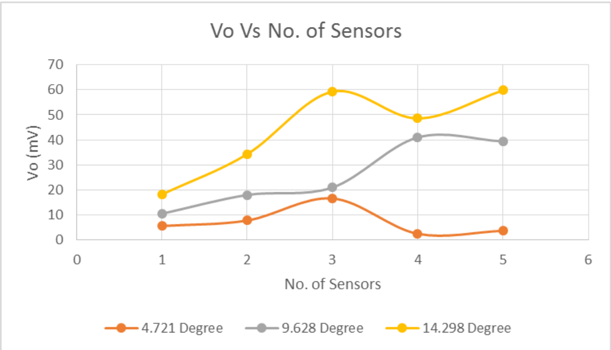

(a)

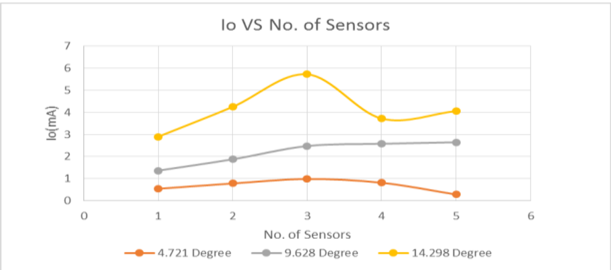

(b)

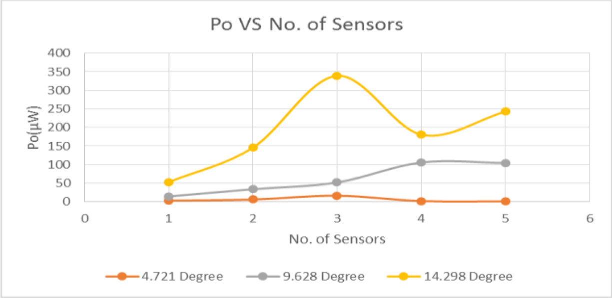

(c)

Fig. 9 Sensors' performance for series configuration: (a) output voltage, (b) output current, and (c) output power against number of sensors

C. Parallel Performance

For the third configuration, the sensors are connected in parallel connection by all possible parallel sequences. By connecting them in parallel connection, the voltage of the sensors is maintained whilst the current is expected to increase linearly. The parallel connection ensures delivery of maximum power through the increment of current rating. The results for parallel configuration are recorded in Table 6(a)-(c) for various temperature differences while Figure 10 illustrates the performance of the sensors against varied number of sensors used in the configuration.

Table 6(a) Sensor parallel configuration for temperature differences at 2.31 °C

No. of Sensor	ΔT (°C)	Vo (mV)	Io (mA)	Po (μW)
1	2.31	5.6	0.55	3.08
2	2.31	4.5	0.85	3.83
3	2.31	1.0	0.22	0.22
4	2.31	1.9	0.33	0.63
5	2.31	2.9	0.54	1.57

Table 6(b) Sensor parallel configuration for temperature differences at 9.31 °C

No. of Sensor	ΔT (°C)	Vo (mV)	Io (mA)	Po (μW)
1	9.31	10.5	1.37	14.39
2	9.31	10.5	2.13	22.37
3	9.31	11.6	2.37	27.49
4	9.31	10.7	2.58	27.61
5	9.31	11.1	2.71	30.08

Table 6(c) Sensor parallel configuration for temperature differences at 15.54 °C

No. of Sensor	ΔT (°C)	Vo (mV)	Io (mA)	Po (μW)
1	15.54	18.2	2.90	52.78
2	15.54	15.4	2.84	43.74
3	15.54	15.9	3.45	54.86
4	15.54	15.4	3.54	54.52
5	15.54	15.2	3.70	56.24

Retrieval Number: B3769079220/2020©BEIESP
DOI:10.35940/ijrte.B3769.079220
Journal Website: www.ijrte.org

Published By:
Blue Eyes Intelligence Engineering
& Sciences Publication

At this juncture, it seems that the performance for parallel configuration has not achieved a lot by linearizing the parameters. However, the current's rise for bigger temperature differences is promising. From the graph in Fig. 10, it is clear that the effect of power generation starts when the temperature difference is over 9.31 °C. Overall, the performance of the series configuration is more stable and generates more power than the paralled configuration.

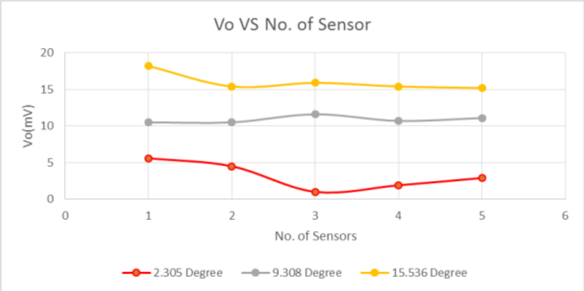

(a)

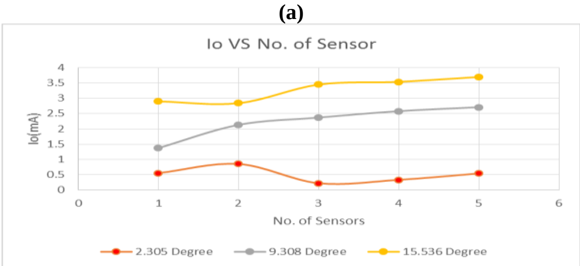

(b)

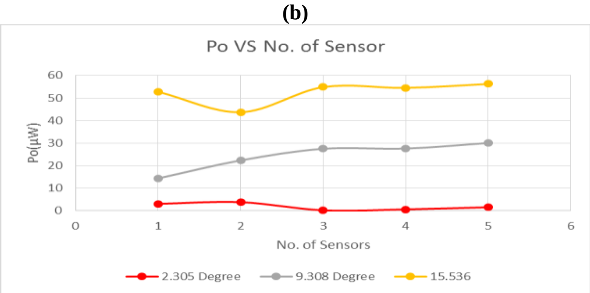

(c)

Fig.10 Sensors' performance for parallel configuration: (a) output voltage, (b) output current, and (c) output power against number of sensors

IV. CONCLUSION AND FUTURE WORKS

The experimental results show that it is feasible to incorporate TEG sensor together with medical sensors to produce a self-sustaining health monitoring system. From the results acquired, the TEG sensor is able to generate up to 242.78 µW of power by configuring it in series with a temperature difference of about 15 °C.

In order to maximize the performance of the sensor, the temperature fluctuation needs to be controlled to prevent the non-linear performance of the output. Assuming that the minimum power requirement is 30 µW, the hot side of the TEG sensor can be coated with a heating element to produce a temperature difference of 15 °C against the human body temperature. Thus, the above condition is proposed to ensure a continuous and stable power generated by the TEG sensor for the medical sensor.

During the experimental stage, the output measurement of the sensor is not appropriate since both the temperatures of the cold and hot sides fluctuate. The hot side of the sensor heated up by the hot plate does not produce uniform heat dissipation to all the sensors while the cold side exposed to the ambient room temperature fluctuates as well with the air conditioner's system. The heat dissipation of the hot plate is illustrated in Fig. 11 for the reference of visual purpose.

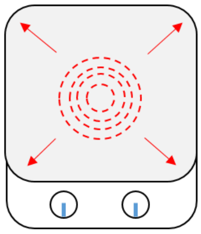

Fig. 11 Heat dissipation of hot plate

Hence, fixing the temperature at the hot side of the TEG sensor is preferred. Moreover, the heat dissipation of a human body is considered not uniform because the surface of the human body is curvy and a TEG sensor will be unable to absorb the maximum heat unless it is specifically fabricated to fully cover the of human body curvature.

As a conclusion, it is feasible to fabricate a TEG sensor and combine it with medical sensors to achieve a self-sustained autonomous system with proper sensor configurations, together with a suitable power conditioning system. The designed power management system must be able to regulate the fluctuated raw outputs from the TEG sensors. The multi-stages charge pump approach that has been proposed in the previous work (appear in [13,14] seems suitable to be used for low-power TEG application as described in this paper.

ACKNOWLEDGMENT

The authors express gratitude to the Malaysian Ministry of Education (MOE) and Universiti Teknologi Malaysia for research grant with vote number 05G03 for supporting this work.

REFERENCES

1. R. Kappel, Pachler, W., Auer, M., Pribyl, W., Hofer G. and Holweg, G. "Using Thermoelectric Energy Harvesting to Power a Self-Sustaining Temperature Sensor in Body Area Network." *IEEE 2013:* 787-792, 2013.
2. A. Montecucco, Siviter, J. and Knox, A.R. "The Effect of Temperature Mismatch on Thermoelectric Generators Connected in Series and Parallel." *Elsevier Journal of Applied Energ.:* 47-54, 2015.
3. A. Chen, "Thermal Energy Harvesting with Themoelectrics for Self-powered Sensors: With Applications to Implantable Medical Devices, Body Sensor Networks and Aging in Place." *Thesis, University of California*, 2011.
4. X. Niu, Yu, J. and Wang, S. "Experimental Study on Low-Temperature Waste Heat Thermoelectric Generator." *Elsevier Journal of Power Sources.* Vol. 188, Issue 2, 15 March 2009: 621-626, 2008.
5. C.J. Udalagama, "Electrical Energy Generation From Body Heat." *IEEE ICSET*, 2010. 6-9 Dec 2010.
6. M.K. Kim, Kim, M.S., Jo, S.E., Kim, H.L., Lee, S.M. and Kim, Y.J. "Wearable Thermoelectric Generator for Human Clothing Applications." *IEEE Transducer 2013*, Barcelona, Spain 16-20 June 2013.
7. Z. Luo, Z. "A Simple Method to Estimate The Physcical Characteristics of A Thermoelectric Cooler," from Vendor Datasheets. *Electronics Cooling*, 2010.

8. D.K. Aswal, R. Basu and A. Singh, "Key issues in development of thermoelectric power generators: Highfigure-of-merit materials and their highly conducting interfaces withmetallic interconnects," Energy Conversion and Management, vol. 114. pp. 50-67, 2016.
9. G. Wu, Yu, X. "System Design on Thermoelectric Energy Harvesting from Body Heat." *39th Annual Northeast Bioengineering Conference*. : 157 – 158, 2013.
10. Q. Brogan, O'Connor, T. and Ha, D.S. "Solar and Thermal Energy Harvesting with a Wearable Jacket." *IEEE*, 2014: 1412 – 1415, 2014.
11. Z.H. Abdul Rahman, Md Khir, M.H., Burhanudin, Z.A., et. al. "CMOS based Thermal Energy Generator For Low Power Devices." *IJSER*, Vol. 4, Issue 5, May 2013.
12. T.M.M.A.I Omer, "Development of Solar Thermoelectric Generator." *European Scientific Journal*, Edition Vol. 10, No. 9, March 2014 : 123 – 134, 2014.
13. C.C. Law, C.C., Wahid, H., Abdul Rahim, H. and Abdul Rahim, R. "A Review of Thermoelectric Energy Harvester and Its Power Management Approach in Electronic Applications." Jurnal Teknologi, Vol. 73(3) : 153-159, 2015.
14. C.C. Law, Wahid, H. and Leow, P.L. (2015). A Charge Pump-based Power Conditioning Circuit for Low Powered Thermoelectric Generator (TEG). The 10th Asian Control Conference 2015, Sabah, Malaysia (appear in IEEE Xplore), 2015.
15. R. Yusof, H. Wahid, M. H. I. Ishak, D. Hanafi, R. Ghazali, "Performance Examination and Design Optimization of Thermoelectric Sensor Configuration for Energy Harvesting From Air Conditioner Waste Heat," International Journal of Recent Technology and Engineering (IJRTE), Vol. 8(3S2), October 2019.

AUTHORS PROFILE

Law Choon Chuan has obtained Bachelor's Degree in Electrical Engineering (Power) in 2014 from Universiti Malaysia Pahang. He is currently pursuing his Master Philosophy studies in Universiti Teknologi Malaysia.

Herman Wahid received the B.Eng. in Electrical Engineering (Instrumentation and Control) in 2000, and M.Eng in Electrical Engineering (Mechatronics and Automatic Control) in 2007 from Faculty of Electrical Engineering, Universiti Teknologi Malaysia (UTM), Malaysia. He then obtained his Ph.D from University of Technology, Sydney (UTS), Australia in 2013. He has five years experience in industry (2000-2005) and is currently a Senior Lecturer in UTM. His research interests include artificial intelligences, controller design and optimization, environmental quality instrumentation and energy harvesting system.

Dirman Hanafi is currently working at Universiti Tun Hussein Onn Malaysia, Johor. His research interest includes Intelligent Control System System, Identification, Artificial Intelligent, Robotics. He is serving as an honorary author for Global Journal of Technology and Optimization. He has authored of several H1 research articles/books related to Control Engineering and Technology. His research interest includes Intelligent Control System, Identification, Artificial Intelligent and Robotics.

Seriaznita Haji Mat Said received the B.Edu. (TESL) from University of Malaya (UM), Malaysia, M.Edu (TESL) from Universiti Putra Malaysia (UPM), Malaysia and Ph.D in TESL from Universiti Teknologi Malaysia (UTM), Malaysia. She is currently a Senior Lecturer in UTM (Kuala Lumpur branch) at Language Academy Center.